Improvement of LVRT Capability of Wind Farms by Using SMES and R-Type BFCL

Masoud Radmehr[1*],Seyyedeh Maral Moharreri koushalshah[2]

Abstract- Fulfillment the Low-voltage ride-through (LVRT) is required for wind farms (WFs) connected to the power system. This paper proposes simultaneous using both superconducting magnetic energy storage (SMES) and R-type solid-state fault current limiter (SSFCL) for enhancement the LVRT capability of WFs. The WFs is modeled with a doubly-fed induction generator (DFIG). The drive-train system is modeled by two-mass drive system. The analytical and simulation studies of using both SCES and R-type SSFCL for improving the LVRT capability of WFs are presented and compared with the impact of the Using the SMES alone. The simulation results show that simultaneous using both SCES and SSFCL effectively improves the LVRT capability of WFs connected to weak grids. Simulation were performed in PSCAD/EMTDC software environment.

Keywords: Low-Voltage Ride-Through (LVRT), superconducting magnetic energy storage (SMES), Solid-state Fault Current Limiter(SSFCL) Wind Farms (WFs).

1. Introduction

Global warming and energy shortage issues have become one of the biggest challenges facing the world [1]. Expanding the capacity of renewable energy generation systems (REGSs) can be the best solution to response these challenges. The wind turbine generation system (WTGS) is one of the reprehensive REGSs. They are harvest from nature, free and clean [1-2]. Installed WTGSs capacity is continuously increasing over the past decade in wind Farms (WFs). Increasing wind power penetration levels has led to the elaboration of specific technical requirements for connection of WFs to the power system, as a part of the grid codes by the transmission system operators (TSOs).In the grid code requirements, low voltage ride through (LVRT) is one of the important and pertinent issues [2]. The ability of WTs to stay connected to the grid during faults and voltage dips is stated as LVRT capability and they are described by a voltage against time characteristic. Different countries have defined different LVRT requirements depend on the WFs penetration level and on the robustness of the power system.

Figure 1 shows the E.ON standard LVRT characteristic that is a popular one and is used in this study. As shown in this figure, the code defines are as follow [2-3]:

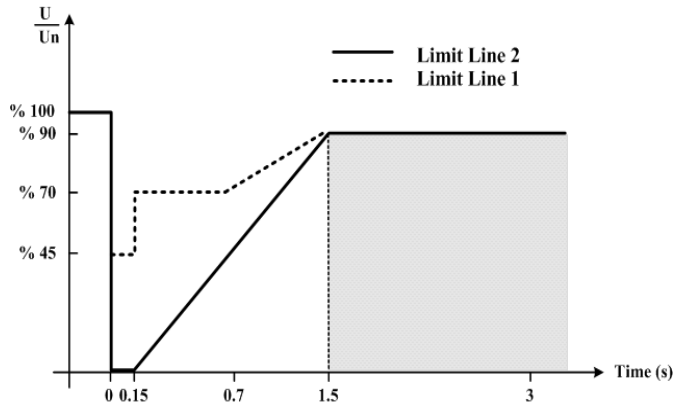

Figure 1: Limit curve for LVRT requirements of E.ON grid code

- Three-phase short circuits or symmetrical voltage dips in WF terminal must not lead to instability above limit line 1 or to disconnection of it.
- Voltage drops within the area between limit line 1 and limit line 2 should not lead to disconnection, but in case of wind turbine instability, short-time disconnection is allowed.
- Below limit line 2 disconnections of the wind turbines is allowed.

To address this challenge, several methods have been proposed and documented, which can be classified as follows:

1* **Corresponding Author :** Department of Electrical Engineering, Aliabad Katoul Branch, Islamic Azad University, Aliabad Katoul, Iran, Email: radmehr.masoud@yahoo.com

2 Department of Electrical Engineering, Aliabad Katoul Branch, Islamic Azad University, Aliabad Katoul, Iran.

Received 2019.12.25 ; Accepted 2020.05.10

- Modification of rotor side converter (RSC) and grid side converter (GSC) control system of the DFIG under fault condition [4-5]
- Using hardware protection schemes such as Static Synchronous Compensator (STATCOM)[6], unified inter-phase power controller (UIPC)[7-8], dynamic voltage restorer (DVR)[9], series dynamic braking resistor (SDBR) [10-11], superconducting magnetic energy storage (SMES) [12-13] and fault current limiter (FCLs) [14-20].

Application of SMES in WFs effectively reduce the output power fluctuations and enhance the LVRT capability of WFs [12-13]. But, using only SMES may be degraded for enhancement of LVRT under severe fault conditions. FCLs were recognized as a promising and cost effective protection scheme for using in WFs for limiting fault current and enhancing the LVRT capability [18-21].

In this paper, the application of both SEMS and R-type SSFCL is proposed for improving LVRT capability of WFs under sever fault condition. Under grid normal operation mode of system, the SMES mitigate the output power fluctuations and the SSFCL has no effects on system performance. Under fault condition, both SSFCL and SMES are activated for enhancing the LVRT capability and fault current contribution of WFs. The Matlab/Simulink software is used in this study.

2. Description of Study System

A single line diagram of study system with SMES and R-type SSFCL is shown in Figure 2. The WF is connected through a 0.69 kV/13.8 kV transformer to a PCC bus and then connected to power system through a 13.8 kV/66 kV step up transformer. It includes 20 wind turbine (2 MW rated). The wind speed is 10m/s and WFs produce 70% of the nominal output power. To investigate the efficacy of SMES and SSFCL performance a three-line-to-ground (3LG) fault is simulated in the study system. The parameters of this system are listed in appendix A.

Figure 3 shows the conventional SSFCL configuration. It consists of diode bridge and a DC reactor and has significant advantages as follow [20]:

A. The fault current limitation without any delay and smoothing the surge current waveform,

B. Prevention from instantaneously deep voltage drop during fault and

C. Capability of controlling the fault current by controlling the DC reactor current.

These characteristics of the conventional SSFCL improve transient behavior of power system over limiting fault current. But, it cannot limit the magnitude of fault current under fault condition.

In [20], a resistor in parallel with a semiconductor switch has been connected in series with the DC reactor as R-type SSFCL. The main purpose of the suggested topology is the reduction of the current rating of the DC reactor and limiting the magnitude of fault current. In this paper, the same topology is used to enhance the LVRT capability of WFs. The proposed R-type SSFCL is shown in Figure 4. The DC reactor of FCL is connected to the secondary winding of the series coupling transformer (Ta, Tb and Tc). The DC reactor has been modeled by rd and L_d, i.e., the resistance and inductance of DC reactor, respectively. The parallel connection of discharging resistor (R) and semiconductor switch (T) are connected in series with the DC reactor [20].

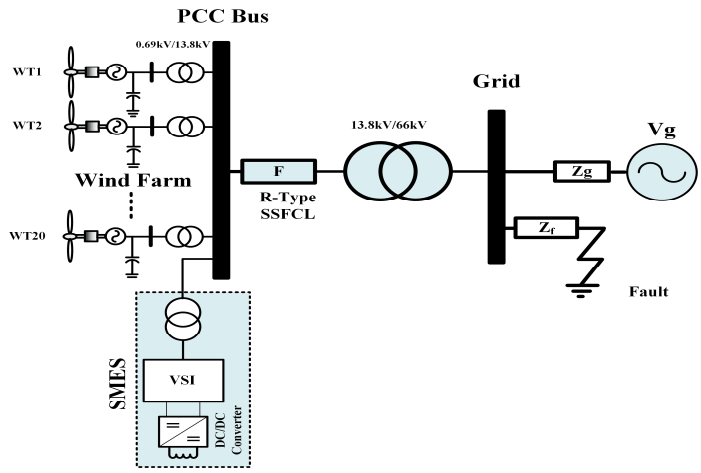

Figure 2: Single line diagram of study system with R-type SSFCL and SMES

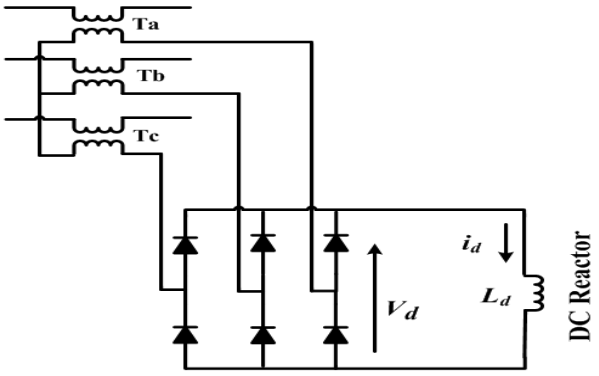

Figure 3: Conventional SSFCL

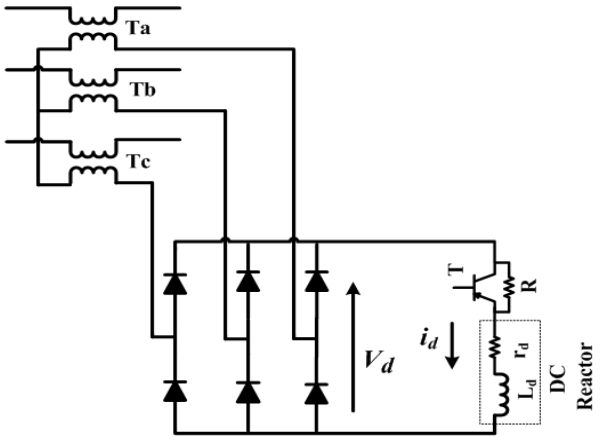

Figure 4: R-type SSFCL

Figure 5 shows the configuration of SMES unit. It is a device that stores energy in the magnetic field that is generated by the dc current flowing through a superconducting coil. The inductively stored energy (in joules) and the rated power (in watts) are commonly given specifications for SMES devices, and they can be expressed as follows:

$$E_{smes} = \frac{1}{2} L_{smes} I_{smes}^2$$

$$P_{smes} = \frac{dE_{smes}}{dt} = L_{smes} I_{smes} \frac{dI_{smes}}{dt} = V_{smes} I_{smes} \quad (1)$$

Since energy is stored as circulating current, energy can be drawn from an SMES unit with almost instantaneous response with energy stored or delivered over periods ranging from a fraction of a second to several hours, more specifications have been given in [21].

SMES coil is connected to the UPFC dc-bus through a dc-dc chopper which controls dc current and voltage levels by converting the UPFC dc bus voltage to the adjustable voltage across the SMES coil terminal. Simple chopper is shown in Figure 4. Chopper operation can be defined as follows:

$$V_{smes} = (1 - 2d) V_{dc} \quad (2)$$

According to (2), it is evident that if d is less than 0.5, the SMES average voltage is positive, consequently chopper will be in charging mode and absorbs the energy and increases the I_{smes}.Vice versa when d is more than 0.5, chopper operates in discharging mode and injects the energy into the power system. Chopper operation will be in standby mode when d is 0.5, the average voltage across SMES coil will be zero, therefore no energy will exchange with power system.

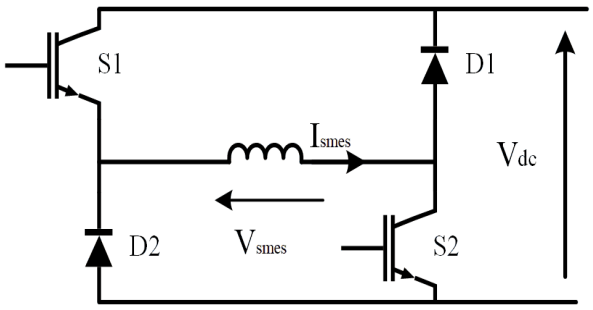

Figure 5: dc-dc converter for integration SMES

3. Results and Discussion

To investigate the capability of SMES and R-type SSFCL, a 3LG fault is simulated on the grid side, which starts at t=10s as shown in Figure 2. After 0.4s, the circuit breaker isolated the fault. The simulations have been carried out by Matlab/Simulink for following cases:

A. **Case A**: Without using any external device

B. **Case B**: With using SMES alone,

C. **Case C**: With using both SMES and R-type SSSFCL.

Figure 6 shows the rotor speed of the DFIG for three cases, respectively. As shown in Fig. 6, the rotor speed gradually reduces to the pre-fault level and the system is stable in both cases B and C, but the DFIG is unstable in case A. Also, in the case C, the SMES and SSFCL provide a better damping to post-fault oscillations.

Figure 7 shows the PCC voltage of IG for three cases. It can be seen that the PCC voltage drops to zero in cases A and B, approximately during fault. After fault clearance in case A, the PCC voltage cannot be restored to pre-fault level. But, in the case C, the PCC voltage sag decreases to 0.8 pu and is restored quickly after the fault clearance compare to case B.

Figures 8 and 9 show the active and reactive power exchanged between the study WF and the grid for three cases, respectively. After the fault, the active power is restored by in cases B and C. As shown in Figure 9, the absorbing reactive power from the grid is significantly reduced in the case C, which helps to restore the PCC voltage quickly after the fault clearance.

Figures 10(a), (b) and (c) demonstrate the DFIG rotor currents for case A, case B and case C, respectively. As

demonstrated from this figure, the rotor current raises to 4 pu at the fault inception time in case A. However, in case B and C, sudden jump in rotor current is effectively limited.

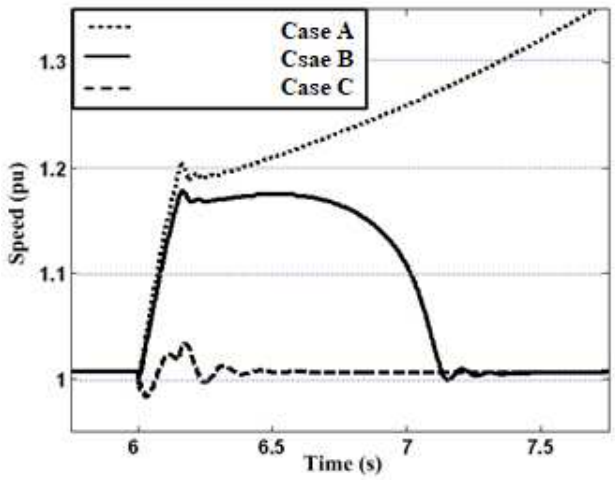

Figure 6: Rotor speed for three cases during fault

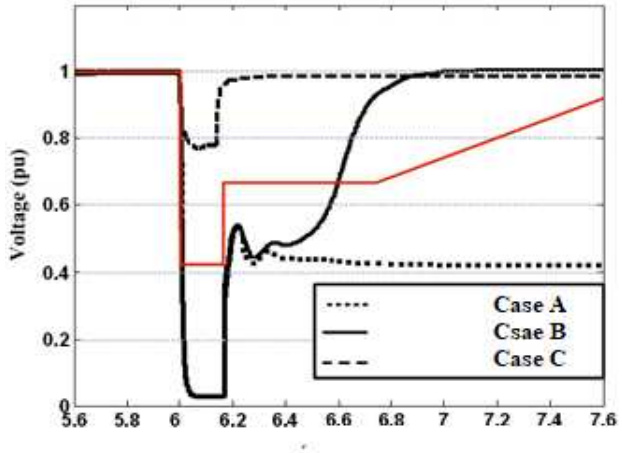

Figure 7: PCC voltage for three cases during fault

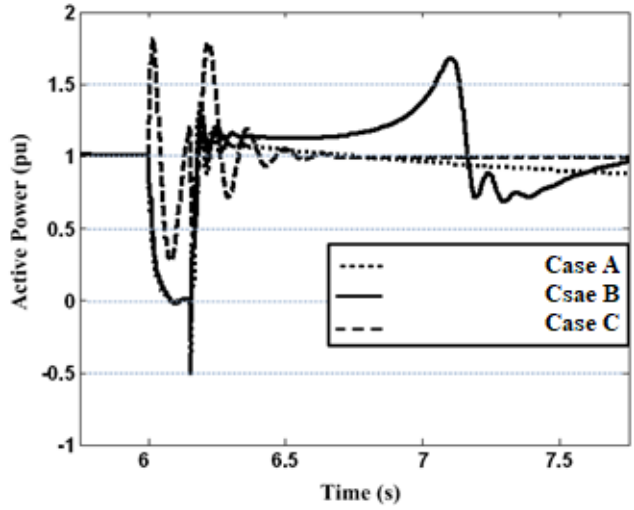

Figure 8: Active power for three cases during fault

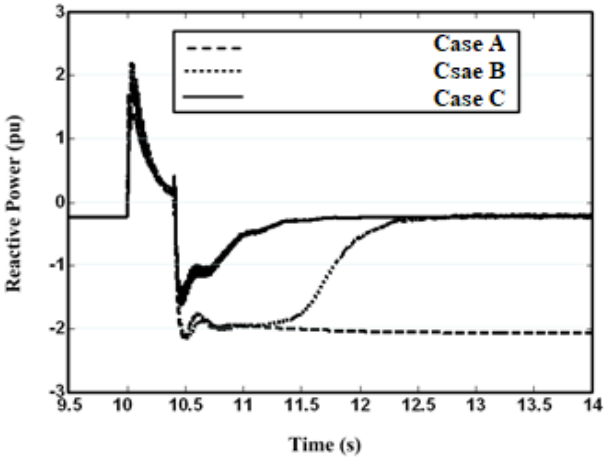

Figure 9: Reactive power for three cases during fault

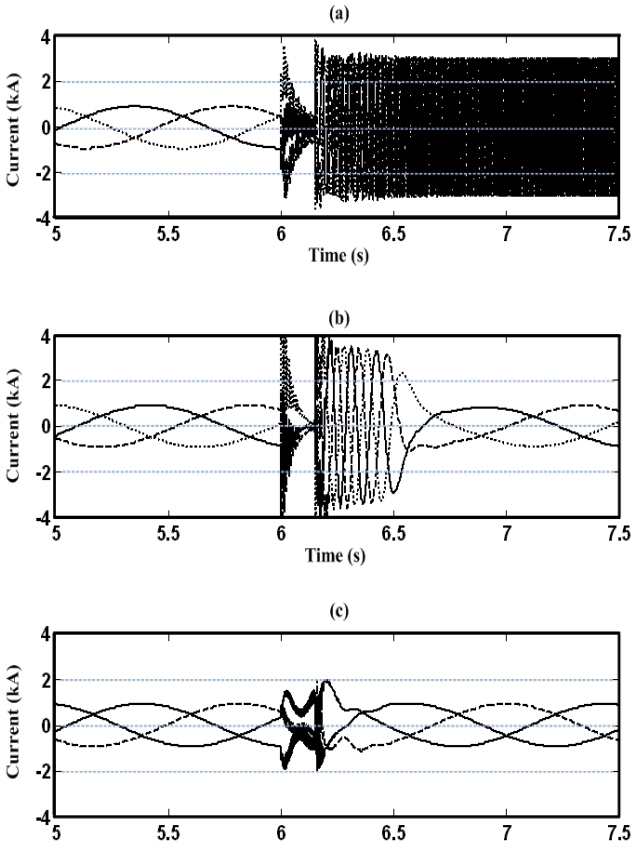

Figure 10: Rotor current (a) Case A, (b) Case B, (c) Case C

4. CONCLUSION

In this paper, the application of simultaneous SMES and SSFCL has been proposed for improving the LVRT capability of WFs. Based on simulation results, the following points can be drawn:

- Under fault condition, the fault current is limited by R-type SSFCL without any delay and prevention from deep voltage drop.
- Also, it improves transient behavior of DFIG-based WF transient performance during fault.
- The comparison with SMES shows that the simultaneous R-type SSFCL and SMES is more effective for enhancement of LRT capability than SMES only.

APPENDIX

GRID PARAMETERS:	
Supply	66 kV
Frequency	50Hz
Step down	13/8kV/66 kV
Transformer	50 MVA
X/R ratio	5
INDUCTION GENERATOR PARAMETERS:	
Number of poles	4
Slip	1.8%
Power factor	0.9
Stator resistance	0.0577 Ω
Rotor resistance	0.0161 Ω
Stator reactance	0.0782 Ω
Rotor reactance	0.012 Ω
Magnetizing reactance	2.43 Ω

References

[1] GWEC. (2010,October)" Global wind energy outlook 2010," in Global Wind Energy Council Report[Online]. Available: http://www.gwec.net.

[2] S. M. Muyeen, R. Takahashi, T. Murata, and J. Tamura, "A variable speed wind turbine control strategy to meet wind farm grid code requirements," IEEE Transactions on power system., Vol. 25, No. 1, PP. 331–340, Feb. 2010.

[3] M. Tsili and S. Papathanassiou, "A Review of Grid Code Technical Requirements for Wind Farms," IET Renewable Power Generation, Vol. 3, No. 12, pp. 308–332, Sep 2009.

[4] S. Tohidi, B. M. Ivatloo, "A comprehensive review of low voltage ride through of doubly fed induction wind generators", Renewable and Sustainable Energy Reviews, Vol. 57, pp. 412-419, May 2016.

[5] K.C. Divya, P.S. N. Rao, "Study of dynamic behavior of grid connected induction generator," IEEE Power Engineering Society General Meeting, 6-10 June 2004, vol.2, pp. 2200-2205

[6] R. C´ardenas, R. Pe˜na, S. Alepuz, and G. Asher, "Overview of control systems for the operation of DFIGs in wind energy applications," IEEE Transaction Industrial Electronic, Vol. 60, No. 7, pp. 2776–2798, Jul. 2013

[7] L. Wang and D.-N. Truong, "Stability enhancement of DFIG-based offshore wind farm fed to a multi-machine system using a STATCOM,"IEEE Trans. Power Syst., vol. 28, no. 3, pp. 2882–2889, Aug. 2013.

[8] M. Firouzi, G. B. Gharehpetian, S. B. Mozafari, "Application of UIPC to improve power system stability and LVRT capability of SCIG-based wind farms" IET Generation, Transmission & Distribution, Vol. 11, No. 9, pp.2314-2322, Jul. 2017

[9] M. Firouzi, G. B. Gharehpetian, Y. Salami," Active and reactive power control of wind farm for enhancement transient stability of multi-machine power system using UIPC" IET Renewable Power Generation, Vol. 11, No. 8, pp.1246-1252, 2017

[10] Ch. Wessels, F. Gebhardt, F. W. Fuchs ," Fault Ride-Through of a DFIG Wind Turbine Using a Dynamic Voltage Restorer During Symmetrical and Asymmetrical Grid Faults ," IEEE Transactions on Power Electronics, Vol. 26, No. 3, pp. 807-815, Feb. 2017.

[11] Kh. Goweily, M. Sh. El Moursi, M. Abdel-Rahman, M. A. L. Badr," Voltage booster scheme for enhancing the fault ride-through of wind turbines "IET Power Electronics, Vol. 8, No. 10, pp. 1853-1863, 2015

[12] J. Yang, J. Fletcher, and J. O'Reilly, "A series-dynamic-resistor-based converter protection scheme for doubly-fed induction generator during various fault conditions," IEEE Trans. Energy Convers., vol. 25, no. 2, pp. 422–432, Jun. 2010.

[13] C. Abbey and G. Joos, "Supercapacitor energy storage for wind energy applications," IEEE Transactions on Industry Applications, vol. 43, no. 3, pp. 763–776, 2007

[14] A. Yazdani, "Islanded operation of a doubly-fed induction generator (DFIG) wind-power system with integrated energy storage," in Proceedings of the 2007 IEEE Canada Electrical Power Conference, EPC 2007, pp. 153–159, Montreal, Canada, October 2007

[15] G. Rashid, and M. H. Ali, "Transient Stability Enhancement of Double Fed Induction Machine Based Wind Generator by Bridge-Type Fault Current Limiter," IEEE Transactions on Energy Conversion , Vol. 30, No. 3, 2015

[16] M. E. Elshiekh, D. E. A. Mansour, and A. M. Azmy, "Improving fault ride-through capability of DFIG-based wind turbine using superconducting fault current

limiter," IEEE Trans. Appl. Supercond.,Vol. 23, no. 3, Jun. 2013, Art. ID. 5601204.

[17] Chen, L.; Deng, C.; Zheng, F.; Li, S.; Liu, Y.; Liao, Y. Fault ride-through capability enhancement of DFIG-based wind turbine with a flux-coupling-type SFCL employed at different locations. IEEE Trans. Appl. Supercond. 2015, 25, Art. no. 5201505.

[18] G. Rashid and M. Hasan Ali, "Bridge-type fault current limiter for asymmetric fault ride-through capacity enhancement of doubly fed induction machine based wind generator," in Proc. IEEE Energy Convers. Congr. Expo., Sep. 2014, pp. 1903–1910.

[19] Salami "Dynamic performance of wind farms with bridge-type superconducting fault current limiter in distribution grid," in Proc. 2nd Int. Conf. Elect. Power Energy Convers. Syst., 2011,pp. 1–6.

[20] M. Firouzi and G. B. Gharehpetian, "Improving Fault Ride-Through Capability of Fixed-Speed Wind Turbine by Using Bridge-Type Fault Current Limiter," IEEE Transactions on Energy Conversion, Vol. 28, No. 2, pp. 361–369, 2013.

[21] N. G. Hingorani, "High power electronics and flexible AC transmission system," IEEE. Power Engineering Review, pp. 3-4, july 1998